Proceedings of 20th International Congress on Acoustics, ICA 2010

23–27 August 2010, Sydney, Australia

The ultra weak variational formulation for 3D elastic wave problems

Teemu Luostari (1), Tomi Huttunen (1) and Peter Monk (2)

(1) Department of Physics and Mathematics, University of Eastern Finland, Kuopio, Finland
(2) Department of Mathematical Sciences, University of Delaware, Newark DE, USA

PACS: 43.58.Ta, 43.20.Bi, 43.40.Fz, 43.20.Gp

ABSTRACT

In this paper we investigate the feasibility of using the ultra weak variational formulation (UWVF) to solve the time-harmonic 3D elastic wave propagation problem. The UWVF is a non-polynomial volume based method that uses plane waves as basis functions which reduces the computational burden. More general, the UWVF is a special form of the discontinuous Galerkin method. As a model problem we consider plane wave propagation in a cubic domain. We shall show numerical results for the accuracy, conditioning and *p*-convergence of the UWVF. In addition, we shall investigate the effect of different ratios of the *P*- and *S*-wave basis functions.

INTRODUCTION

Elastic wave problems, in common with acoustic and electromagnetic problems, are usually challenging and computationally demanding due to the need approximate wavelike solutions. An added difficulty for elastic waves is that the solutions consist of two components, S and P-waves, with different wave numbers. Therefore it is useful to develop numerical methods that reduces the computational time, and also which can approximate the S and P waves separately.

The approach we follow is to use non-polynomial basis functions that are appropriate solutions of the underlying equation (for other applications of non-polynomial basis functions see (Barnett and Betcke 2010, Cessenat and Després 1998, Gabard 2007, Farhat et al. 2001, Huttunen et al. 2002, Perrey-Debain 2006)). The analysis and implementation of methods based on non-polynomial bases is an active area of research and these methods have been compared to each other recently, see, for example, references (Gabard et al. 2010, Gamallo and Astley 2007, Huttunen et al. 2009). However, the 3D elasticity problem has not been considered to date, and we shall focus on the ultra weak variational formulation (UWVF) for the 3D elastic wave problems.

The UWVF was first developed for the Helmholtz and Maxwell equations by Cessenat and Després, see references (Cessenat 1996, Cessenat and Després 1998). Further development, and particularly computational aspects of the UWVF for acoustics and electromagnetism, can be found in (Huttunen et al. 2007a;b, Loeser and Witzigmann 2009). Relevant to this paper is the study of the UWVF for the 2D elastic wave problems investigated in reference (Huttunen et al. 2004).

The UWVF is a volume based method that uses plane wave basis functions which are efficient to compute. However, if too many plane wave basis functions are used on an element the results may become inaccurate due to the ill-conditioning. Therefore, in this paper we study the behavior of the 3D elastic UWVF with different numbers of basis functions, and different ratios between S and P-wave components. The UWVF is a special form of the discontinuous Galerkin method, shown independently in references (Huttunen et al. 2007a, Gabard 2007). Thus the UWVF shares similar properties with the DGM and similar finite element meshes are used in the UWVF. In addition, convergence analysis of the non-polynomial DGM, shown in references (Hiptmair et al. 2009, Gittelson et al. 2009), are then applicable for the UWVF. The error estimates for the UWVF has been studied in reference (Buffa and Monk 2008). No estimates are specifically available for 3D elasticity. In this paper we aim to show preliminary numerical results for accuracy, *p*-convergence and conditioning of the 3D elastic UWVF.

This paper is organized as follows: First we give a short introduction of the UWVF for the Navier equation of elasticity with discretization. A detailed derivation of the 2D elastic UWVF, which is similar to 3D, can be found in reference (Huttunen et al. 2004). In the second section we show the numerical results for the model problem which is plane wave propagation in a cubic domain. Finally we draw conclusions from the preliminary numerical experiments.

THE ULTRA WEAK VARIATIONAL FORMULATION

In this section we consider the ultra weak variational formulation for the Navier equation, and its discretization by plane waves.

The UWVF for the Navier equation

Let K be a computational domain with the boundary $\Gamma = \partial K$ and let us assume that K consists of non-overlapping elements, i.e. $K = \cup_{k=1}^{N} K_k$ where N is the number of elements (a finite element grid). We consider the Navier equation

$$\mu\Delta\mathbf{u} + (\lambda+\mu)\nabla(\nabla\cdot\mathbf{u}) + \omega^2\rho\mathbf{u} = 0 \quad \text{in } K_k \tag{1}$$

where ω is the angular frequency of the field, $\mathbf{u}$ is the time-harmonic displacement vector, λ and μ are the Lamé constants and ρ is the density of the medium. Later we use the following notation $\Delta^e = \mu\Delta\mathbf{u} + (\lambda+\mu)\nabla(\nabla\cdot\mathbf{u})$. The Lamé constants can be expressed as

$$\mu = \frac{E}{2(1-\nu)} \quad \text{and} \quad \lambda = \frac{E\nu}{(1+\nu)(1-2\nu)}, \tag{2}$$

where E is the Young's modulus and ν is the Poisson ratio.

Next we define the traction operator $\mathbf{T}^{(\mathbf{n})}(\mathbf{u})$ on any closed surface C so that

$$\mathbf{T}^{(\mathbf{n})}(\mathbf{u}) = 2\mu\frac{\partial \mathbf{u}}{\partial \mathbf{n}} + \lambda\mathbf{n}\nabla\cdot\mathbf{u} + \mu\mathbf{n}\times\nabla\times\mathbf{u}. \tag{3}$$

where $\mathbf{n}$ is an outward unit normal to the surface C, see (Huttunen et al. 2004).

The complex conjugate (denoted by overline) of the traction operator $\mathbf{T}$ is defined as follows

$$\overline{\mathbf{T}^{(\mathbf{n})}}(\mathbf{u}) = 2\overline{\mu}\frac{\partial \mathbf{u}}{\partial \mathbf{n}} + \overline{\lambda}\mathbf{n}\nabla\cdot\mathbf{u} + \overline{\mu}\mathbf{n}\times\nabla\times\mathbf{u}. \tag{4}$$

In addition we note that

$$\overline{\overline{\mathbf{T}^{(\mathbf{n})}}(\mathbf{u})} = 2\mu\frac{\partial \overline{\mathbf{u}}}{\partial \mathbf{n}} + \lambda\mathbf{n}\nabla\cdot\overline{\mathbf{u}} + \mu\mathbf{n}\times\nabla\times\overline{\mathbf{u}}. \tag{5}$$

The boundary condition on the exterior boundary Γ can be written as

$$\mathbf{T}^{(\mathbf{n})}(\mathbf{u}) - i\sigma\mathbf{u} = Q(-\mathbf{T}^{(\mathbf{n})}(\mathbf{u}) - i\sigma\mathbf{u}) + g \quad \text{on } \Gamma \tag{6}$$

where g is the source term, $\mathbf{n}$ is an outward unit normal, σ is a coupling parameter (flux parameter) and $Q \in \mathbb{C}$, $|Q| \leq 1$ defines the type of the boundary conditions.

A time-harmonic elastic plane wave (solution of the Navier equation) moving in a direction $\mathbf{d}$ in free space can be expressed as

$$\begin{aligned}\mathbf{u} =& A_1\mathbf{d}\exp(i\kappa_P\mathbf{d}\cdot\mathbf{x}) + A_2\mathbf{d}_{SH}\exp(i\kappa_S\mathbf{d}\cdot\mathbf{x}) \\ &+ A_3\mathbf{d}_{SV}\exp(i\kappa_S\mathbf{d}\cdot\mathbf{x})\end{aligned} \tag{7}$$

where $\mathbf{d}_{SH} = \mathbf{d}^{\perp}$, $\mathbf{d}_{SV} = \mathbf{d}^{\perp}\times\mathbf{d}$, wave numbers $\kappa_P = \omega/c_P$ and $\kappa_S = \omega/c_S$ (wave speeds c_P and c_S will be specified later) and A_1, A_2 and A_3 are amplitudes. In the equation (7) the first component is called a P-wave and denoted $\mathbf{u}_P$, and the second two components are S-waves (SH-wave $\mathbf{u}_{SH}$ and SV-wave $\mathbf{u}_{SV}$, respectively). In addition, the following conditions hold $\nabla\times\mathbf{u}_P = 0$ and $\nabla\cdot\mathbf{u}_{SH} = \nabla\cdot\mathbf{u}_{SV} = 0$.

The wave speed c_P for the P-wave is

$$c_P = \sqrt{\frac{\lambda + 2\mu}{\rho}} \tag{8}$$

and the wave speed c_S for S-waves (SH- and SV-waves) is

$$c_S = \sqrt{\frac{\mu}{\rho}}. \tag{9}$$

Therefore waves can propagate with different speeds. Fortunately, in the UWVF we can define the number of basis functions separately for P-waves and S-waves which balances the method (limiting the growth of ill-conditioning). Now we give a short introduction to the derivation of the UWVF for the Navier equation. However, the detailed derivation of the UWVF can be found in (Huttunen et al. 2004). Let us denote $\mathbf{u}_k := \mathbf{u}|_{K_k}$ and let the solution $\mathbf{u}_k$ of Navier equation satisfy

$$\Delta^e\mathbf{u}_k + \omega^2\rho\mathbf{u}_k = 0 \quad \text{in } K_k \tag{10}$$

where Δ^e represents the differential operator in (1) such that

$$\mathbf{T}^{(\mathbf{n})}(\mathbf{u}_k) - i\sigma\mathbf{u}_k \in (L^2(\partial K_k))^3. \tag{11}$$

Similarly let $\mathbf{e}_k$ be a test function that satisfies

$$\Delta^e\overline{\mathbf{e}}_k + \omega^2\rho\overline{\mathbf{e}}_k = 0 \quad \text{in } K_k \tag{12}$$

such that

$$\overline{\mathbf{T}^{(\mathbf{n})}}(\mathbf{e}_k) - i\sigma\mathbf{e}_k \in (L^2(\partial K_k))^3. \tag{13}$$

Using a straightforward extension of the "Isometry Lemma", the UWVF for the Navier equation in 2D proved in reference (Huttunen et al. 2004) , the UWVF for the 3D Navier equation can now be written as

$$\begin{aligned}&\sum_k\int_{\partial K_k}\sigma^{-1}\mathscr{X}_k\cdot\overline{(-\overline{\mathbf{T}^{(\mathbf{n}_k)}}(\mathbf{e}_k) - i\sigma\mathbf{e}_k)} \\ &\quad -\sum_k\sum_j\int_{\Sigma_{kj}}\sigma^{-1}\mathscr{X}_j\cdot\overline{(\overline{\mathbf{T}^{(\mathbf{n}_k)}}(\mathbf{e}_k) - i\sigma\mathbf{e}_k)} \\ &\quad -\sum_k\int_{\Gamma_k}Q\sigma^{-1}\mathscr{X}_k\cdot\overline{(\overline{\mathbf{T}^{(\mathbf{n}_k)}}(\mathbf{e}_k) - i\sigma\mathbf{e}_k)} \\ &\quad =\sum_k\int_{\Gamma_k}\sigma^{-1}g\cdot\overline{(\overline{\mathbf{T}^{(\mathbf{n}_k)}}(\mathbf{e}_k) - i\sigma\mathbf{e}_k)}\end{aligned} \tag{14}$$

where $\mathscr{X}_k = \mathbf{T}^{(\mathbf{n}_k)}(\mathbf{u}_k) - i\sigma\mathbf{u}_k$ on ∂K_k. Here we shall consider the following flux parameter σ by defining

$$\sigma = \omega\rho\mathbb{R}\{c_P\}I \tag{15}$$

where $\mathbb{R}\{c_P\}$ indicates the real part of c_P and I is the unit matrix (other choices of σ are possible, see Huttunen et al. (2004)). Flux parameter in equation (15) is an ad hoc choice and the optimal flux parameter will be investigated later.

Discretization

We use the Helmholtz decomposition for the solution of the adjoint Navier equation by separating it into three components: P-wave, SH-wave and SV-wave (see also above). Therefore

$$\mathbf{e}_k = \mathbf{e}_{k,P} + \mathbf{e}_{k,SH} + \mathbf{e}_{k,SV} \tag{16}$$

in which the following conditions hold $\nabla\times\mathbf{e}_P = 0$ and $\nabla\cdot\mathbf{e}_{SH} = \nabla\cdot\mathbf{e}_{SV} = 0$.

Using the same decomposition as in equation (16) we can write the approximation for $\mathscr{X}_k$ as follows

$$\begin{aligned}\mathscr{X}_k \approx &\sum_{\ell=1}^{p_P^k}\left[x_{k,\ell}^P\left(-\mathbf{T}^{(\mathbf{n}_k)}(\mathbf{e}_{k,\ell}^P) - i\sigma\mathbf{e}_{k,\ell}^P\right)\right] \\ &+\sum_{\ell=1}^{p_S^k}\left[x_{k,\ell}^{SH}\left(-\mathbf{T}^{(\mathbf{n}_k)}(\mathbf{e}_{k,\ell}^{SH}) - i\sigma\mathbf{e}_{k,\ell}^{SH}\right)\right] \\ &+\sum_{\ell=1}^{p_S^k}\left[x_{k,\ell}^{SV}\left(-\mathbf{T}^{(\mathbf{n}_k)}(\mathbf{e}_{k,\ell}^{SV}) - i\sigma\mathbf{e}_{k,\ell}^{SV}\right)\right]\end{aligned} \tag{17}$$

where p_P^k is the number of basis functions for P-wave, p_S^k respectively for SH- and SV-waves and

$$\mathbf{e}_{k,\ell}^P = \begin{cases}\mathbf{a}_{k,\ell}\exp(i\overline{\kappa}_P\mathbf{a}_{k,\ell}\cdot\mathbf{x}) & \text{in } K_k \\ 0 & \text{elsewhere}\end{cases}$$

$$\mathbf{e}_{k,\ell}^{SH} = \begin{cases}\mathbf{a}_{k,\ell}^{\perp}\exp(i\overline{\kappa}_{SH}\mathbf{a}_{k,\ell}\cdot\mathbf{x}) & \text{in } K_k \\ 0 & \text{elsewhere}\end{cases}$$

$$\mathbf{e}_{k,\ell}^{SV} = \begin{cases}\mathbf{a}_{k,\ell}^{\perp}\times\mathbf{a}_{k,\ell}\exp(i\overline{\kappa}_{SV}\mathbf{a}_{k,\ell}\cdot\mathbf{x}) & \text{in } K_k \\ 0 & \text{elsewhere}\end{cases}$$

where $\mathbf{a}_{k,\ell}$ is the direction of propagation. This defines a discrete space of traces on the skeleton of the mesh that we denote $V_{h,k}$.

Now we can write the discrete UWVF by finding $\mathscr{X}_{h,k} \in V_{h,k}$, $k = 1, 2, \ldots, N$ such that

$$\begin{aligned}&\sum_k\int_{\partial K_k}\sigma^{-1}\mathscr{X}_{h,k}\cdot\overline{\mathscr{Y}_{h,k}} - \sum_k\sum_j\int_{\Sigma_{kj}}\sigma^{-1}\mathscr{X}_{h,j}\cdot\overline{F_k(\mathscr{Y}_{h,k})} \\ &-\sum_k\int_{\Gamma_k}Q\sigma^{-1}\mathscr{X}_{h,k}\cdot\overline{F_k(\mathscr{Y}_{h,k})} = \sum_k\int_{\Gamma_k}\sigma^{-1}g\cdot\overline{F_k(\mathscr{Y}_{h,k})}\end{aligned} \tag{18}$$

for all $\mathscr{Y}_{h,k} \in V_{h,k}, k = 1,2,\ldots,N$. Where the operator F is defined element by element by

$$
\begin{aligned}
F_k(\mathscr{Y}_{h,k}) \approx & \sum_{\ell=1}^{p_P^k} \left[y_{k,\ell}^P \left(\mathbf{T}^{(\mathbf{n}_k)}(\mathbf{e}_{k,\ell}^P) - i\sigma \mathbf{e}_{k,\ell}^P \right) \right] \\
& + \sum_{\ell=1}^{p_S^k} \left[y_{k,\ell}^{SH} \left(\mathbf{T}^{(\mathbf{n}_k)}(\mathbf{e}_{k,\ell}^{SH}) - i\sigma \mathbf{e}_{k,\ell}^{SH} \right) \right] \\
& + \sum_{\ell=1}^{p_S^k} \left[y_{k,\ell}^{SV} \left(\mathbf{T}^{(\mathbf{n}_k)}(\mathbf{e}_{k,\ell}^{SV}) - i\sigma \mathbf{e}_{k,\ell}^{SV} \right) \right]. \qquad (19)
\end{aligned}
$$

The discrete elastic UWVF can be written in a matrix form as follows

$$(D - C)X = b \qquad (20)$$

where D corresponds to the first sesquilinear form on the left hand side of (18) and C to the second term. We shall see shortly that D is block diagonal, so we actually use the numerically more stable form

$$(I - D^{-1}C)X = D^{-1}b \qquad (21)$$

where D and C are sparse block matrices and $X = (x_{11}^P, \ldots, x_{1p_1}^P, x_{11}^{SH}, \ldots, x_{1s_1}^{SH}, x_{11}^{SV}, \ldots, x_{1s_1}^{SV}, \ldots)^T$. The block matrix D may become ill-conditioned if too many basis functions are used in small elements. Therefore it is essential to examine the conditioning of the UWVF problem.

The matrix D is a Hermitian diagonal block matrix as

$$
D = \begin{pmatrix}
D^1 & 0 & \ldots & \ldots & \ldots & \ldots & 0 \\
0 & D^2 & 0 & \ldots & \ldots & \ldots & 0 \\
\vdots & 0 & \ddots & 0 & \ldots & \ldots & 0 \\
\vdots & \vdots & 0 & D^k & 0 & \ldots & 0 \\
\vdots & \vdots & \vdots & 0 & \ddots & 0 & 0 \\
\vdots & \vdots & \vdots & \vdots & 0 & \ddots & 0 \\
0 & 0 & 0 & 0 & 0 & 0 & D^N
\end{pmatrix}, \qquad (22)
$$

where

$$
D^k = \begin{pmatrix}
D_{P,P,\ell,m}^k & D_{SH,P,\ell,m}^k & D_{SV,P,\ell,m}^k \\
D_{P,SH,\ell,m}^k & D_{SH,SH,\ell,m}^k & D_{SV,SH,\ell,m}^k \\
D_{P,SV,\ell,m}^k & D_{SH,SV,\ell,m}^k & D_{SV,SV,\ell,m}^k
\end{pmatrix}. \qquad (23)
$$

For example, $D_{P,SH,\ell,m}^k$ in (23) is of the form

$$
\begin{aligned}
& D_{P,SH,\ell,m}^k = \\
& \int_{\partial K_k} \sigma^{-1} \left(-\mathbf{T}^{(\mathbf{n}_k)}(\mathbf{e}_{k,m}^P) - i\sigma \mathbf{e}_{k,m}^P \right) \cdot \overline{\left(-\mathbf{T}^{(\mathbf{n}_k)}(\mathbf{e}_{k,\ell}^{SH}) - i\sigma \mathbf{e}_{k,\ell}^{SH} \right)}, \\
& \qquad (24)
\end{aligned}
$$

with similar expressions for other blocks of the matrix.

Matrix C consists of blocks C^k and $C^{k,j}$ (will be given shortly). Matrix blocks C^k are on the diagonal and $C^{k,j}$ are on the off-diagonal of matrix C. Matrix block C^k can be written as follows

$$
C^k = \begin{pmatrix}
C_{P,P,\ell,m}^k & C_{SH,P,\ell,m}^k & C_{SV,P,\ell,m}^k \\
C_{P,SH,\ell,m}^k & C_{SH,SH,\ell,m}^k & C_{SV,SH,\ell,m}^k \\
C_{P,SV,\ell,m}^k & C_{SH,SV,\ell,m}^k & C_{SV,SV,\ell,m}^k
\end{pmatrix} \qquad (25)
$$

where, for example, $C_{P,SH,\ell,m}^k$ is of the form

$$
\begin{aligned}
& C_{P,SH,\ell,m}^k = \\
& \int_{\Gamma_k} Q\sigma^{-1} \left(-\mathbf{T}^{(\mathbf{n}_k)}(\mathbf{e}_{k,m}^P) - i\sigma \mathbf{e}_{k,m}^P \right) \cdot \overline{\left(\mathbf{T}^{(\mathbf{n}_k)}(\mathbf{e}_{k,\ell}^{SH}) - i\sigma \mathbf{e}_{k,\ell}^{SH} \right)}, \\
& \qquad (26)
\end{aligned}
$$

similarly others. The off-diagonal block matrix $C^{k,j}$ is as follows

$$
C^{k,j} = \begin{pmatrix}
C_{P,P,\ell,m}^{k,j} & C_{SH,P,\ell,m}^{k,j} & C_{SV,P,\ell,m}^{k,j} \\
C_{P,SH,\ell,m}^{k,j} & C_{SH,SH,\ell,m}^{k,j} & C_{SV,SH,\ell,m}^{k,j} \\
C_{P,SV,\ell,m}^{k,j} & C_{SH,SV,\ell,m}^{k,j} & C_{SV,SV,\ell,m}^{k,j}
\end{pmatrix} \qquad (27)
$$

where, for example, $C_{P,SH,\ell,m}^{k,j}$ is of the form

$$
\begin{aligned}
& C_{P,SH,\ell,m}^{k,j} = \\
& \int_{\Sigma_{kj}} \sigma^{-1} \left(\mathbf{T}^{(\mathbf{n}_k)}(\mathbf{e}_{j,m}^P) - i\sigma \mathbf{e}_{j,m}^P \right) \cdot \overline{\left(\overline{\mathbf{T}^{(\mathbf{n}_k)}}(\mathbf{e}_{k,\ell}^{SH}) - i\sigma \mathbf{e}_{k,\ell}^{SH} \right)}, \\
& \qquad (28)
\end{aligned}
$$

others can be derived in a similar manner.

NUMERICAL RESULTS FOR THE 3D ELASTIC WAVE PROBLEM

We investigate the UWVF for the 3D elastic wave problem. We consider a simple 3D model problem, plane wave propagation in a unit cube. The exact solution is of the form

$$
\begin{aligned}
\mathbf{u} = & A_1 \mathbf{d} \exp(i\kappa_P \mathbf{x} \cdot \mathbf{d}) + A_2 \mathbf{d}_{SH} \exp(i\kappa_S \mathbf{x} \cdot \mathbf{d}) \\
& + A_3 \mathbf{d}_{SV} \exp(i\kappa_S \mathbf{x} \cdot \mathbf{d}) \qquad (29)
\end{aligned}
$$

where the direction of plane wave propagation is chosen in our simulations as $\mathbf{d} \approx [-0.73 \quad 0.45 \quad 0.51]$, $|\mathbf{d}| = 1$, $\mathbf{d}_{SH} = \mathbf{d}^{\perp}$, $\mathbf{d}_{SV} = \mathbf{d}^{\perp} \times \mathbf{d}$ and the amplitudes $A_1 = A_2 = A_3 = 1$. We emphasize that the incident direction $\mathbf{d}$ is not equal of any directions used in the basis functions. As a boundary condition we choose an impedance type boundary condition, i.e. $Q = 0$ in equation (6). In the following simulations uniform/structured meshes are used because we want to investigate the convergence of the method. However, it is, of course, possible to use unstructured/non-uniform meshes where the element sizes vary and in the UWVF the number of basis functions can vary from element to element as well.

In the first numerical study we investigate the elastic UWVF with different wave numbers. The mesh size and the number of basis functions are fixed and the wave numbers vary. The mesh is shown in Figure 1 and the number of basis functions per element for the P-wave is $p_P = 37$ and for the S-waves $p_S = 43$ (the total number of basis functions per element is $p_{tot} = p_P + 2p_S$ because there are horizontal and vertical S-waves (i.e. SH- and SV-waves)). As physical material parameters we have Young's modulus $E = 70 \cdot 10^9$, Poisson ratio $\nu = 0.33$, the density $\rho = 2700$ and the wave speeds c_P=6.1978e3 and c_S = 3.1220e3.

Results are shown in Table 1. There relative errors are computed as discrete L2-error such as

$$\text{error}(\%) = \frac{||u_{ex} - u_{UWVF}||_{\ell^2}}{||u_{ex}||_{\ell^2}} \times 100\% \qquad (30)$$

where the exact solution u_{ex} and the UWVF solution u_{UWVF} are computed in a dense set of uniformly distributed points (number of points is 40401).

These results show that when the wave numbers increase the errors increase as expected. In addition, when the wave numbers increase, the maximum of the element-wise condition number of the matrix D decreases when the number of basis functions is fixed. This is also observed in other problems.

In practice, there are three possibilities to enhance the accuracy, one is to refine the mesh size and the second is to increase the number of basis functions and the third is to proceed changing

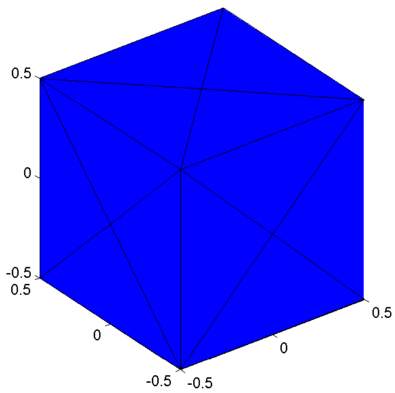

Figure 1: The mesh used in the first numerical model problem. The computational domain consists of 24 tetrahedra and 14 vertices.

Table 1: Behavior of the UWVF when the wave number varies and the mesh size and the number of basis functions are fixed. The number of basis functions for P-wave $p_P = 37$ and for S-wave $p_S = 43$ (total number of basis functions per element is $p_{tot} = p_P + 2p_S$). The maximum of the elementwise condition number of D matrix is denoted by max(cond(D^k)).

κ_P	κ_S	error(%)	max(cond(D^k))
5.0689	10.0629	0.2125	7.5017e7
7.0964	14.0881	1.2807	1.4313e6
8.1102	16.1007	2.8948	2.9047e5

both, i.e. refine the mesh size and increase the number of basis functions.

Next we shall study numerically the effects of changing the number of basis function and the ratio of basis functions between P- and S-waves. The aim of this study is to find the optimal ratio between the basis functions. We note that theoretical and numerical studies of optimal ratios of the basis function ratios in the plane wave based methods can be found in reference (Perrey-Debain 2006). Five cases are herein considered when the wave numbers are $\kappa_P = 4.0551$ and $\kappa_{SH} = \kappa_{SV} = 8.0503$, the angular frequency $\omega = 0.8\pi \cdot 10^4$, Young's modulus $E = 70 \cdot 10^9$, Poisson ratio $\nu = 0.33$ and the density $\rho = 2700$, the wave speeds c_P=6.1978e3 and c_S = 3.1220e3, the number of basis function ratios are $p_P = 0.25p_S$, $p_P = \frac{1}{3}p_S$, $p_P = 0.5p_S$, $p_P = \frac{2}{3}p_S$ and $p_P = p_S$ where p_P is the number of basis functions for the P-wave and p_S is the number of basis functions for the S-wave. Notice that the total number of basis functions per element is $p_{tot} = p_P + 2p_S$ because there are SH- and SV-waves. The mesh used in this simulation is shown in Figure 1. The mesh consists of 24 tetrahedra elements. Results of the p-convergence and the conditioning are shown in Figure 2.

The results show that there is an impact of using different ratios between the number of basis functions for P- and S-waves. However, the slopes does not differ much with different basis function ratios. Results suggest that when the number of basis functions (p_P) for P-wave approaches to the number of S-wave basis functions (p_S) the condition number for D grows which is plausible since the wave number for P-wave is smaller that the wave number for S-wave. The best conditioning is obtained by choice $p_P = p_S/3$. Taking $p_P/p_S \approx \kappa_P/\kappa_{SH}$ gives similar conditioning as choice $p_P = p_S/3$ but the error is less effected by this choice.

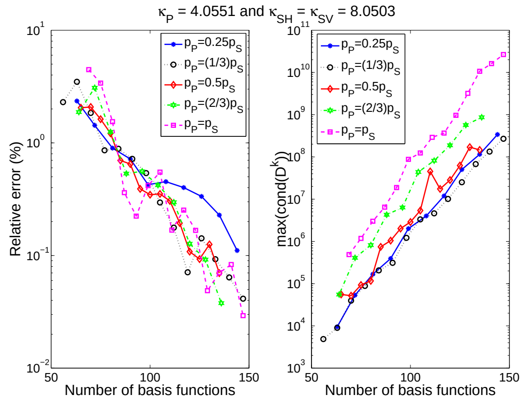

Figure 2: Convergence figure for the 3D-elastic-UWVF when $\kappa_P = 4.0551$ and $\kappa_{SH} = \kappa_{SV} = 8.0503$, the mesh size is fixed and the number of basis functions varies. Left panel: the relative error (%) versus the number of basis functions per element, i.e. $p_P + 2p_S$. Right panel: the maximum of the element-wise condition number of the D matrix, i.e. max(cond(D^k)) versus the number of basis functions per element.

CONCLUSIONS

We have shown the feasibility of the UWVF for the 3D Navier equation. In the simulations shown in this paper we used a uniform mesh with the same number of basis functions on each element. In the first test simulation the results show that the mesh size and the number of basis functions have an impact to the accuracy as well as the conditioning. In the second simulation the convergence of the method as the number of basis functions, and the ratio between basis function components, is investigated. The results show that the curves have similar slopes but depending on the basis function ratio the conidition-ing varied. However, more tests are needed to obtain an optimal ratio between the basis functions which ensures accurate results with low cost and small condition number. In addition testing on more complex problems, including those involving surface waves, is needed.

REFERENCES

Alex H. Barnett and Timo Betcke. An exponentially convergent nonpolynomial finite element method for time-harmonic scattering from polygons. *SIAM Journal on Scientific Computing*, 32:1417–1441, 2010.

Annalisa Buffa and Peter Monk. Error estimates for the ultra weak variational formulation of the helmholtz equation. *ESAIM: M2AN Mathematical Modelling and Numerical Analysis*, 42(6):925–940, 2008.

Olivier Cessenat. *Application d'une nouvelle formulation variationnelle aux équations d'ondes harmoniques. Problèmes de Helmholtz 2D et de Maxwell 3D.* PhD thesis, Université Paris IX Dauphine, 1996.

Olivier Cessenat and Bruno Després. Application of an ultra weak variational formulation of elliptic PDEs to the two-dimensional Helmholtz problem. *SIAM Journal on Numerical Analysis*, 35(1):255–299, 1998.

Charbel Farhat , Isaac Harari, and Leopoldo P. Franca. A discontinuous enrichment method. *Computer Methods in Applied Mechanics and Engineering*, 190(48):6455–6479, 2001.

Gwenael Gabard. Discontinuous Galerkin methods with plane waves for time-harmonic problems. *Journal of Computational Physics*, 225(2):1961–1984, 2007.

Gwenael Gabard, Pablo Gamallo, and Tomi Huttunen. A comparison of wave-based discontinuous Galerkin, ultra-weak and least-square methods for wave problems. *Submitted*, 2010.

Pablo Gamallo and Jeremy Astley. Comparison of two Trefftz-type methods: the ultraweak variational formulation and the least-squares method, for solving shortwave 2-D Helmholtz problems. *International Journal for Numerical Methods in Engineering*, 71(4):406–432, 2007.

Claude J. Gittelson, Ralf Hiptmair, and Ilaria Perugia. Planewave discontinuous Galerkin methods: Analysis of the h-version. *ESAIM: M2AN Mathematical Modelling and Numerical Analysis*, 43(2):297–331, 2009.

Ralf Hiptmair, Andrea Moiola, and Ilaria Perugia. Plane wave discontinuous Galerkin methods for the 2D Helmholtz equation: Analysis of the p-version. *SAM-ETHZurich Report 2009-20*, 20:1–20, 2009.

Tomi Huttunen, Peter Monk, and Jari P. Kaipio. Computational aspects of the ultra-weak variational formulation. *Journal of Computational Physics*, 182(1):27–46, 2002.

Tomi Huttunen, Peter Monk, Francis Collino, and Jari P. Kaipio. The ultra weak variational formulation for elastic wave problems. *SIAM Journal on Scientific Computing*, 25(5):1717–1742, 2004.

Tomi Huttunen, Matti Malinen, and Peter Monk. Solving Maxwell's equations using the ultra weak variational formulation. *Journal of Computational Physics*, 223(2):731–758, 2007a.

Tomi Huttunen, Eira T. Seppälä, Ole Kirkeby, Asta Kärkkäinen, and Leo Kärkkäinen. Simulation of the transfer function for a head-and-torso model over the entire audible frequency range. *Journal of Computational Acoustics*, 5(4): 429–448, 2007b.

Tomi Huttunen, Pablo Gamallo, and Jeremy Astley. Comparison of two wave element methods for the helmholtz problem. *Communications in Numerical Methods in Engineering*, 25(1):35–52, 2009.

Martin Loeser and Bernd Witzigmann. The ultra weak variational formulation applied to radiation problems with macroscopic sources in inhomogeneous domains. *IEEE Journal of Selected Topics in Quantum Electronics*, 15(4): 1144–1155, 2009.

Emmanuel Perrey-Debain. Plane wave decomposition in the unit disc: Convergence estimates and computational aspects. *Journal of Computational and Applied Mathematics*, 193:140–156, 2006.